ENCIT 2018

17th Brazilian Congress of Thermal Sciences and Engineering
November 25th-28th, 2018, Águas de Lindóia, SP, Brazil

ENCIT-2018-0250
COMPUTATION OF A LAMINAR DIFFUSION ETHYLENE/AIR FLAME CONSIDERING SOOT FORMATION AND THE WEIGHTED-SUM-OF-GRAY-GASES MODEL

Luís Gustavo Pires Rodrigues
Francis Henrique Ramos França
Fernando Marcelo Pereira
Federal University of Rio Grande do Sul, Mechanical Engineering Department, Porto Alegre, RS, Brazil
lgustavo.prodrigues@gmail.com
frfranca@mecanica.ufrgs.br
fernando.pereira@ufrgs.br

Paulo R. Pagot
CENPES/PDEP/TPP – PETROBRAS – Petroleo Brasieiro S.A.
pagot@petrobras.com.br

Abstract. *In the present study the weighted-sum-of-gray-gases (WSGG) model was coupled with the commercial CFD package Ansys/Fluent to solve a laminar diffusion ethylene/air flame. Numerical data was obtained through the solution of the full transport equations considering detailed chemistry and soot formation. Mixture WSGG coefficients for constant partial pressure ratio (p_w/p_c = 1) were combined with coefficients for soot for 2, 3 and 4 gray gases to account the gas-phase/soot heat transfer. The coupling of the radiation model with the CFD code was made with user-defined functions (UDF) written in C programming language. Fluent standard WSGG model was also applied. The predicted radiant fraction for the Fluent WSGG model implementation was in order of 9% while the UDF implemented WSGG considering 4 gray gases for soot reached up to 13%. The radiative heat flux and radiative heat source computed with Fluent WSGG are considerably lower than the predicted with the UDF implemented WSGG.*

Keywords: *Radiative heat transfer, WSGG model, Computational fluid dynamics (CFD), Laminar diffusion flame, Thermal radiation*

1. INTRODUCTION

Thermal radiation is one of the most important heat transfer mechanisms in combustion devices due to the high temperatures involved. For hydrocarbon fuels combustion product gases such as H_2O and CO_2 participates in the heat exchanges by absorbing and emitting radiant energy. One of the most challenging aspects of thermal radiation modeling consists in the very irregular behavior of the radiative absorption coefficient of the participating species in relation to the wavenumber reaching to hundreds of thousands spectral absorption lines as shown in Figure 1. Besides the line-by-line (LBL) integration that considers all the lines in the species spectra, for practical engineering applications it can become unviable due to the high computational efforts and time. Alternatively, the use of global models such as the spectral line-based weighted-sum-of-gray-gases (SLW), full spectrum k (FSK) and the weighted-sum-of-gray-gases (WSGG) may give sufficiently accurate results with lower computational costs (Solovjov *et al.*, 2017; Maurente *et al.*, 2017; Dorigon *et al.*, 2013).

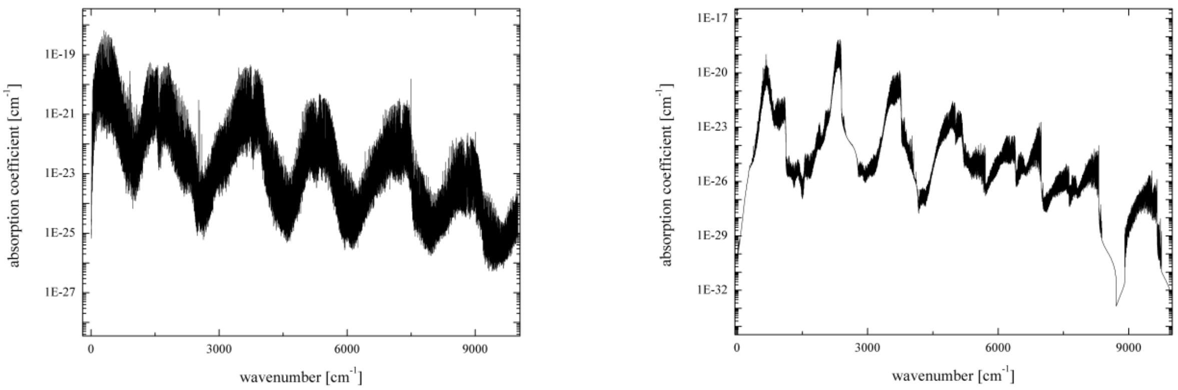

Figure 1. H_2O and CO_2 absorption spectra for T = 1000 K and partial pressure of 0.1 *atm*, respectively.

Sivathanu and Gore (1997) presented a numerical and experimental study of a laminar methane/air flame. Thermal radiation and soot kinetics were considered. Soot volume fractions were measured with the Laser-Induced Incandescence (LII) technique. Results showed that the local heat loss is important for predict local soot volume fractions even for weakly radiating flames. McEnnally et al., 1998, presented a numerical and experimental study of soot formation in a laminar non-premixed ethylene flame. The fuel was diluted with N_2 in order to lift the flame. Measurements of temperature, species concentrations and soot volume fraction were made by both probe and optical diagnostics. Thermal radiation was considered through the optically thin approximation (OTA). Radiative losses were found to have significant impact over the numerical predicted temperature. Smooke et al., 2004, studied the effect of N_2 dilution level on fuel stream over the soot characteristics. Experimental measurements included laser diagnostics and probe techniques. Numerical model included the OTA approximation for radiative losses. Computed flame heights, temperature and soot volume fraction showed good agreement with experimental measurements. Liu *et al.*, 2004, accessed the effects of the radiation model on flame structure. Soot was considered through an acetylene-based semi-empirical two-equation model. Thermal radiation was computed with the statistical narrow band correlated-k model (SNBCK) and the OTA. Results showed that the OTA approximation overpredicts radiative losses, resulting in underestimated temperatures. Also, the effect of radiation absorption showed unimportant when compared to more sooting flames. Smooke et al., 2005, studied the effect of N_2 dilution level on fuel stream over the soot characteristics. Measurements of soot volume fraction were made with LII technique. Numerical predictions were improved with the use of the exponential wide-band (EWB) model for considering radiation reabsorption. The radiative losses showed significant impact over temperature and soot formation. Demarco *et al.*, 2013, investigated the radiation effect on soot formation in laminar diffusion flames for C1-C3 hydrocarbon fuels. Were studied normal and inverse flames in conditions of normal and microgravity. Thermal radiation was computed through the SNBCK model, the OTA approximation and the full spectrum correlated-k (FSCK) model. Results showed that it's necessary to consider the radiative heat transfer to accurately predict temperature and soot concentration. Cao *et al.*, 2015, investigated the influence of fuel dilution, inlet velocity and gravity on laminar diffusion methane flames. Gas-phase detailed chemistry and a sectional aerosol equations soot model were considered. Thermal radiation was accounted with the OTA model. Results showed that the fuel mass flow rate has a major effect and the fuel dilution and inlet velocity are secondary. Ma *et al.*, 2015, presented an experimental and numerical study of methane jet flames in micro and normal gravity conditions. Detailed chemistry with a sectional model for soot was considered. Thermal radiation was treated with the OTA model. Results showed that microgravity flames are sootier than normal gravity flames. Due to the higher radiative losses, the microgravity flames temperatures are lower than normal flames. The OTA model underpredicted soot volume fraction specially for microgravity flames. To accurately predict soot temperature and volume fraction, radiation reabsorption models must be introduced.

In this work a laminar non-premixed coflowing ethylene/air flame was solved with the commercial CFD (computational fluid dynamics) package Ansys/Fluent considering soot formation and soot/gas-phase radiative transfer by coupling UDF (user-defined functions) (Ansys, 2017a) for the WSGG model with recently published coefficients for gas mixtures (Dorigon *et al.*, 2013) and soot (Cassol *et al.*, 2014). Fluent standard WSGG model (Ansys, 2017b) implementation was also considered. Results for radiant fraction, radiative heat flux and radiative heat source are compared in order to investigate the soot radiation and modeling influences on the thermal behavior of the flame.

2. PROBLEM STATEMENT

The problem under investigation consists of a laminar coflowing ethylene/air non premixed flame for which experimental and numerical data are available (Smooke *et al*., 2004; Smooke *et al*., 2005). The domain geometry was kept the same as presented by Connelly *et al.*, 2009, in which fuel is injected by a 0.002 *m* inner radius tube with a wall thickness of 0.00038 *m* (suppressed from the computational domain). The coflow annulus has a 0.037 *m* radius and the domain was radially extended up to 0.04 *m*. A schematic of the domain geometry is presented in Figure 2.

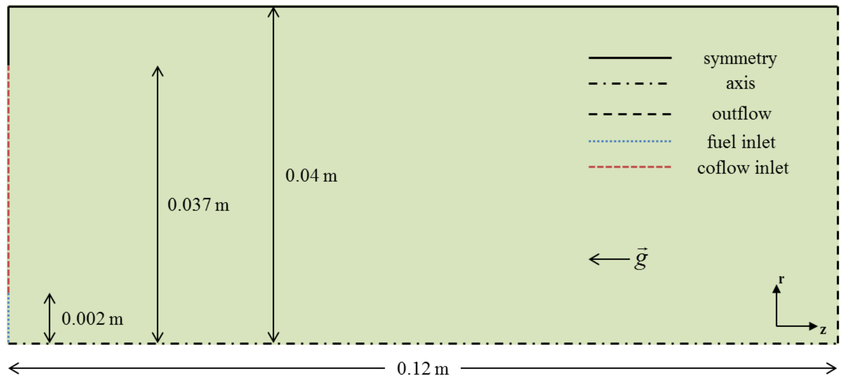

Figure 2. Domain geometry, boundaries and dimensions.

For radiation computations the side boundary was treated as blackbody with prescribed temperature of 298 *K*. The air coflow is composed of 20.9% O_2 (in volume) and N_2 and is injected at a velocity of 0.35 *m/s*. The fuel is composed of a mixture of C_2H_4 (60% in volume) and N_2 and is injected at a velocity of 0.35 *m/s*. A fully developed laminar parabolic velocity profile was considered, given by:

$$v(r) = 2v_{fuel}\left[1-\left(\frac{r}{R}\right)^2\right] \quad (1)$$

where *R* is the fuel inlet radius. Both fuel and coflow air are kept at a temperature of 298 *K*.

2.1 Reactive flow modeling

The reactive flow modeling was made through the conservation equations for the mass (continuity), *momentum*, species mass and energy, respectively:

$$\vec{\nabla}\cdot\left(\rho\vec{v}\right) = 0 \quad (2)$$

$$\vec{\nabla}\cdot\left(\rho\vec{v}\times\vec{v}\right) = \rho\vec{g} + \vec{\nabla}\cdot\hat{\tau} \quad (3)$$

$$\vec{\nabla}\cdot\left(\rho\vec{v}Y_i\right) = -\vec{\nabla}\cdot\vec{J}_i + \dot{\omega}_i\text{, for}\quad i = 1,\ N_s - 1 \quad (4)$$

$$\vec{\nabla}\cdot\left(\rho\vec{v}h\right) = -\vec{\nabla}\cdot\vec{J}_q + \dot{q}_R \quad (5)$$

The low Mach number approximation was assumed and the specific mass was computed as a function of the temperature solely. The shear stress tensor, $\hat{\tau}$, in Eq. (3), was computed with the Stoke's law for Newtonian fluids. The species mass fluxes, $\vec{J}_i$, in Eq. (4), were computed with the Fick's law. The heat flux vector, $\vec{J}_q$, in Eq. (5), was computed considering the Fourier's law and the mass diffusion flux. All transport coefficients for the mixture were computed on a mixture-averaged basis. The transport and thermophysical properties of the individual species were taken from CEMKIN's database. Soot formation was considered through the Fluent's standard implementation of the Moss-Brookes model (Ansys, 2017b).

The chemical source term, $\dot{\omega}_i$, in Eq. (4), was modeled with the Arrhenius kinetic equations. The GRI-Mech 1.2 chemical mechanism was adopted to describe the elementary reactions. The radiative source term, $\dot{q}_R$, in Eq. (5), represents the scope of the present work and will be discussed in the next subsection.

2.2 Radiation modeling

The WSGG model (Hottel and Sarofim, 1967) considers that the integration of the radiative properties of the medium over the spectrum can be replaced for by a summation over a finite number of gray gases. The radiative transfer equation (RTE) derived for the WSGG model is:

$$\frac{dI_j}{dS} = -\kappa_{m,j} I_j + \kappa_{m,j} a_{m,j}(T) I_b(T) \tag{6}$$

in which I_j is the radiative intensity of the *j*-th gray gas, I_b is the blackbody radiation intensity given by the Planck's law. The mixture absorption coefficient, $\kappa_{m,j}$, and the weighting factor, $a_{m,j}$, for the *j*-th gray gas are given by:

$$\kappa_{m,j} = \kappa_{g,j_g} + \kappa_{s,j_s} \tag{7}$$

$$a_{m,j}(T) = a_{g,j_g}(T) \times a_{s,j_s}(T) \tag{8}$$

where the index *g* designates the gas mixture (composed of H_2O and CO_2) and the *s* index designates the soot. The weighting factor can be approximated by a polynomial function of the temperature (Modest, 1991) as follows:

$$a_{\chi,j_\chi}(T) = \sum_{i=1}^{I_\chi} b_{j_\chi,i} T^{i-1} \tag{9}$$

for which $\chi = g$ for the H_2O/CO_2 gas mixture and $\chi = s$ for soot. The absorption coefficients for the gas mixture and soot are computed as:

$$\kappa_{g,j_g} = \kappa_{p,j_g}\left(p_{H_2O} + p_{CO_2}\right) \tag{10}$$

$$\kappa_{s,j_s} = \kappa_{f_v,j_s} \alpha f_v \tag{11}$$

in which p_{H_2O} and p_{CO_2} are the participating species partial pressures, $\alpha = 4.1$ and f_v is the soot volumetric fraction. The weighting factor polynomial coefficients, $b_{j_g,i}$, and the pressure-based absorption coefficients, κ_{p,j_g}, for the gas mixture were taken from Dorigon *et al.*, 2013, for partial pressure ratios $p_w/p_c = 1$. The weighting factor polynomial coefficients, $b_{j_s,i}$, and the volumetric fraction absorption coefficients, κ_{f_v,j_s}, for soot were taken from Cassol et al., 2014, for 2, 3 and 4 gray gases. The total number of gray gases for the gas mixture and soot is $J_m = (J_g + 1) \times J_s$.

The Fluent's standard WSGG, on the other hand, considers a gray form of the RTE where the medium is treated as a single gray gas (i.e. $J_m = 1$). The absorption coefficient for the soot/gas-phase mixture is given by:

$$\kappa = \kappa_g + \kappa_s = -\frac{\ln(1-\varepsilon)}{s} + b_1 \rho_s Y_s \left[1 + b_T (T - 2000)\right] \tag{12}$$

in which $s = 3.6V/A$, with A being the total area of the fluid boundaries and V the fluid volume. Y_s is the soot mass fraction, and $\rho_s = 2000\ kg/m^3$. The constants are $b_1 = 1232.4\ m^2/kg$ and $b_T = 4.8 \times 10^{-6}\ K^{-1}$. The medium total emittance, ε, is computed as:

$$\varepsilon = \sum_{j=0}^{I_g} a_j(T)\left(1 - e^{-\kappa_{p,j} pS}\right) \tag{13}$$

Once the RTE is solved the link with the energy conservation equation is made through the negative of the divergence of the heat flux:

$$\dot{q}_R = \sum_{j=1}^{J_m} -\vec{\nabla}\cdot\vec{q}''_{R,\mathrm{j}} = \sum_{j=1}^{J_m} \kappa_{m,j}\left[\left(\int_{4\pi} I_j d\Omega\right) - 4\pi a_{m,j} I_b\right] \tag{14}$$

3. NUMERICAL CONSIDERATIONS

The resulting set of algebraic equations was solved with the CFD Ansys/Fluent version 18.0. The pressure/velocity coupling was made through the SIMPLE algorithm. Spatial discretization was carried out with the second order upwind scheme for the advective terms and with the central difference scheme for the diffusive terms (Ansys, 2017b).

To reduce the chemistry integration time the ISAT (in-situ adaptive tabulation) and the Chemistry Agglomeration tool were adopted (Ansys 2017b). After the reactive flow stabilization the direct integration of the chemical term was adopted to reach the problem convergence (set as 10^{-5} for all equations).

The angular discretization for the discrete ordinates (DO) method was verified following the *GCI* (grid convergence index) approach (Roache, 1994; Celik et al., 2008). Three angular divisions were adopted for the θ and ϕ angles, $N_\theta = N_\phi = 6,\ 12,\ 24$ (named M3, M2 and M1 respectively). The interest variable chosen was the radiant fraction, X_r, obtained with the Fluent standard WSGG, computed as:

$$X_r = \frac{2\pi R\Delta z}{\dot{m}PCI}\sum_i q''_{R,i} \tag{15}$$

where R is the domain radius, Δz the distance between samples, $\dot{m}$ the mass flow rate and PCI the fuel lower heating value. Table 1 presents the obtained results for the GCI index and the asymptotic range of convergence, χ .

Table 1. *GCI* index and asymptotic range of convergence.

GCI_{12}	GCI_{23}	χ
2.81703E-04	1.67195E-03	1.001112

It can be noticed from Table 1 that the GCI_{12} parameter has an adequate accuracy level. The results close to unity for the χ factor indicates that the solution obtained is within the asymptotic range of convergence. Then, the discrete ordinates M1 division with 24 θ and ϕ control angles was assumed appropriate to carry the radiation computations.

4. RESULTS AND DISCUSSIONS

In this chapter computations carried with the Fluent standard WSGG model will be referred as Fluent WSGG and the computations carried with the classical formulation of the WSGG model implemented via UDF will be referred as UDF WSGG. The converged fields obtained with the solution of the full transport equations for the coupled reactive flow/thermal radiation problem are shown in Figure 3. The radiative transfer was treated using the Fuent WSGG model. These fields were used to carry the computations with the remaining radiation approaches considering the UDF WSGG for soot with 2, 3 and 4 gray gases.

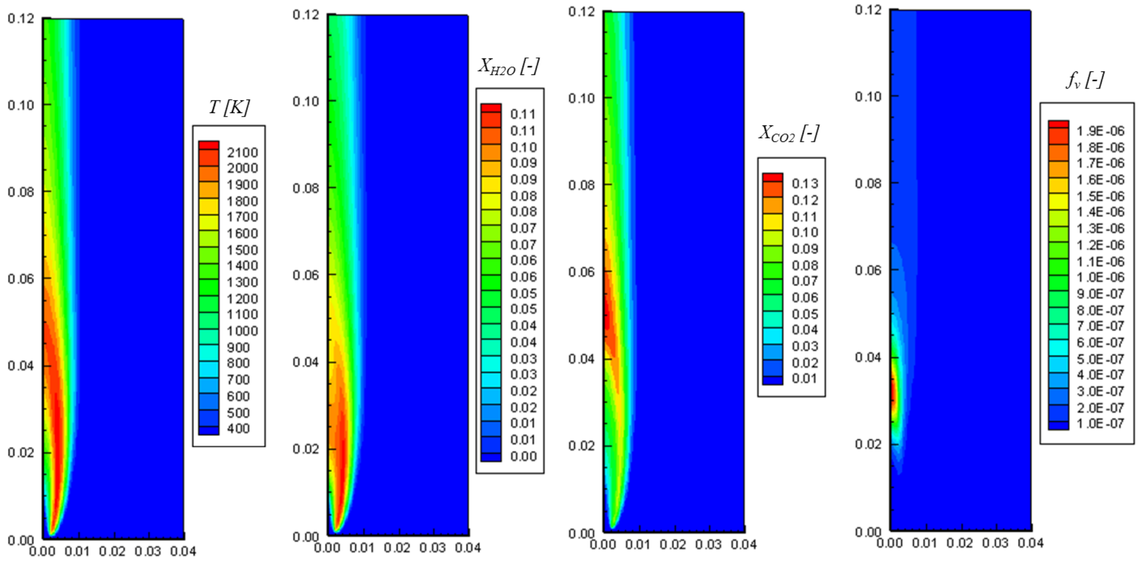

Figure 3. Converged fields of temperature, H_2O mole fraction, CO_2 mole fraction and soot volume fraction, respectively.

Although the goal of this work is not to model accurately soot formation in a flame but investigate the effect of different approaches for radiative transfer modeling, some comparisons with experimental data for the flame centerline temperature (Smooke et al., 2004) and soot volume fraction (Smooke et al., 2005) were made, as shown in Figure 4 and Table 2, respectively.

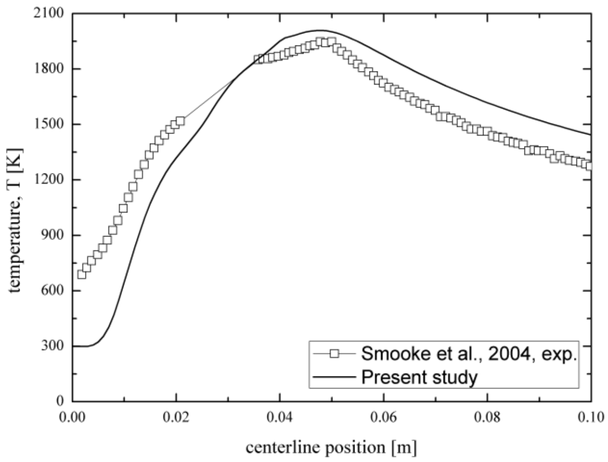

Figure 4. Comparison between numerical computed centerline temperature and literature reported experimental measurements.

As it can be seen computations are in good agreement with experimental measurements for the centerline temperature. Numerical temperature underestimates the experimental in the beginning of the flame and overestimates in the region above.

Table 2. Literature experimental and present study numerical peak soot volume fractions.

f_v peak, exp.	f_v peak, num.	f_v centerline peak, exp.	f_v centerline peak, num.
1.59799×10^{-06}	1.99925×10^{-06}	1.04853×10^{-06}	1.99892×10^{-06}

From Table 2 can be seen that the overall peak soot volume fraction is in good agreement with experimental measurements, with a relative deviation of 25.110%. However the centerline peak presented a larger relative deviation of 90.640%. For future works a more detailed and accurate soot model should be included in the solution.

The results for the side boundary radiative heat flux and centerline radiative heat source for Fluent WSGG and UDF WSGG are shown in Figure 5.

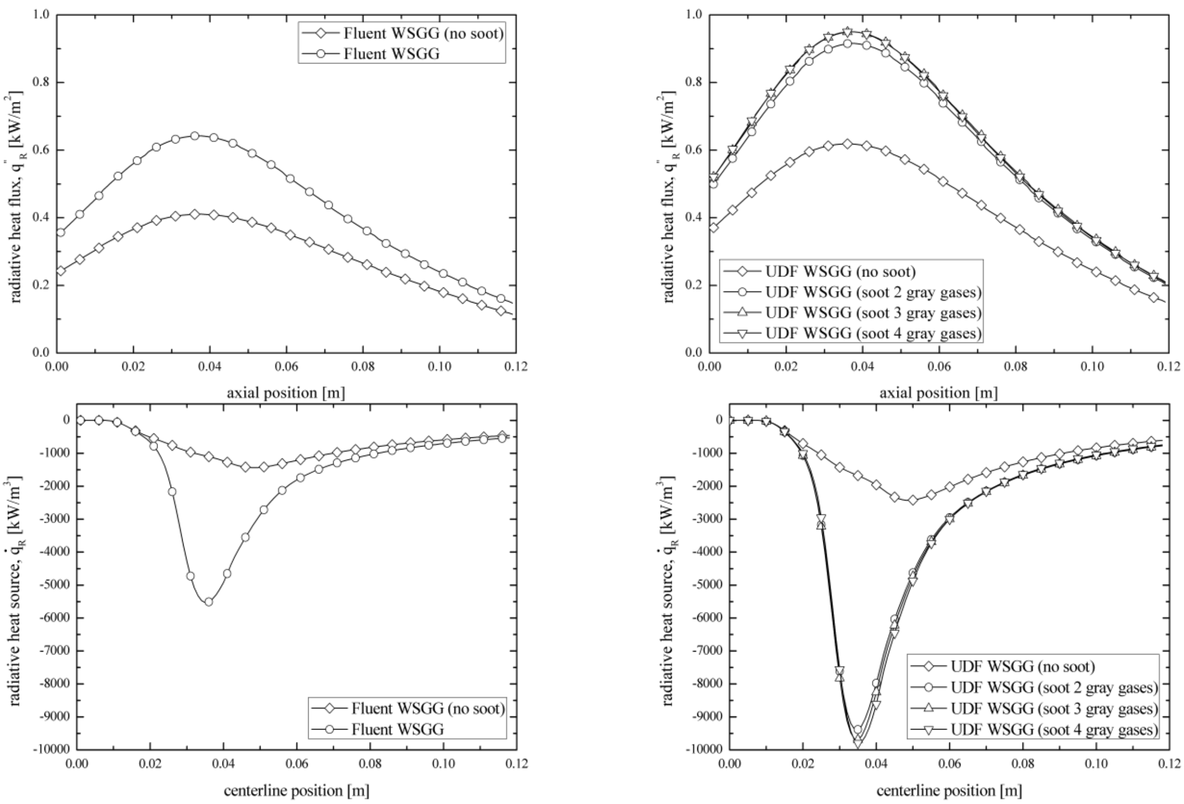

Figure 5. Side boundary radiative heat flux and centerline radiative heat source for all thermal radiation modeling approaches.

It can be noticed from the computed radiative fluxes and sources that the soot radiation contribution must be considered to model the radiation heat transfer for this flame. Fluent WSGG radiative fluxes are considerably lower than UDF WSGG ones. Even when soot contribution is neglected for the UDF WSGG, the computed Fluent WSGG fluxes are lower. This behavior comes from the gray treatment given by the model for the medium absorption coefficient. The UDF WSGG approaches considering 3 and 4 gray gases presented very similar results for both radiative flux and source, but with different computational times: for 3 gray gases $J_m = 15$ while for 4 gray gases $J_m = 20$. Fluent discrete ordinates model for 2D axisymmetric computations considers a total of $4 \times N_\theta \times N_\phi$ directions (Ansys, 2017b) for each gray gas of the mixture, resulting in a total of 34560 and 46080 radiative transfer equations to be solved for $J_m = 15$ and $J_m = 20$, respectively. The radiative heat source computed considering soot is much higher than when no soot is considered and its peak is slightly shifted to the region where soot volume fraction is higher. To quantify the soot importance on heat transfer, the radiant fraction was computed for all implemented approaches considering and not considering soot radiation. Results are shown in Table 3.

Table 3. Computed radiant fractions for all radiation modeling approaches.

	Fluent WSGG	UDF WSGG (no soot)	UDF WSGG (soot 2 gray gases)	UDF WSGG (soot 3 gray gases)	UDF WSGG (soot 4 gray gases)
$X_r\,[\%]$	$X_r\,[\%]$	$X_r\,[\%]$	$X_r\,[\%]$	$X_r\,[\%]$	$X_r\,[\%]$
6.216	9.148	9.080	12.976	13.428	13.407

It can be noticed from Table 3 that the radiant fraction for Fluent WSGG are considerably lower than UDF WSGG computed ones. Soot radiation represents in order of 67% of radiation released and dominates the radiative heat transfer. Fluent WSGG predicts a radiant fraction of 9% while for UDF WSGG the values reach up to 13%. Again the consideration of 3 or 4 gray gases for soot treatment gives very similar results with the first having considerably lower computational costs. Thus, the consideration of a more detailed radiation treatment both for gas-phase and soot radiation are important to accurately predict the radiation heat transfer and, in consequence, flame structure and soot formation.

5. CONCLUSIONS

Three UDF routines were developed to couple with the Fluent solver the WSGG model to account gas-phase and soot radiation. WSGG model correlations for a mixture of constant partial pressure ratio $p_w/p_c = 1$ (Dorigon et al., 2013) were combined with soot correlations for 2, 3 and 4 gray gases (Cassol et al., 2014). An ethylene with N2 dilution (40% by volume) flame was solved (Smooke et al., 2004; Smooke et al., 2005) using the Fluent standard WSGG and the Moss-Brookes model for soot formation (Ansys, 2017b). The converged fields for temperature, H_2O and CO_2 mole fraction and soot volumetric fraction were used to carry decoupled computations for the developed UDF.

Computed results for flame centerline temperature and soot peak volume fraction were compared to literature experimental measurements and showed reasonably accuracy despite the radiation and soot simpler modeling. Computations neglecting soot radiation (i. e., considering only gas-phase radiation) were carried to access soot contribution to the radiative heat transfer. Both Fluent WSGG and UDF WSGG results pointed to the predominance of the soot radiation increasing considerably the radiative heat flux and radiative heat source. Fluent WSGG values for both heat flux and source are significantly lower than the ones computed with UDF WSGG.

Radiant fraction computations quantified the soot importance for the heat transfer in this flame reaching approximately 67% of the total radiant energy released for all approaches (Fluent WSGG and UDF WSGG considering 2, 3 and 4 gray gases for soot). Fluent WSGG computed radiant fraction was in order of 9% while for UDF WSGG this value reached up to 13%. The UDF WSGG approach considering 3 and 4 gray gases for soot radiation presented very similar results for all computed quantities (radiative heat flux and source and radiant fraction), but with considerably lower computational cost for the first approach (where 34560 RTE are solved against 46080 for the second approach). Finally, a more accurate soot formation modeling should be coupled to solve sooting flames on Fluent CFD, also as the radiation modeling must be modified via UDF to give a more realiable treatment for both gas-phase and soot radiation.

6. ACKNOWLEDGEMENTS

The first author in this work thanks to CAPES (Brazil) due to financial support by means of a Doctor Degree scholarship. The third author thanks CNPq (Brazil) for research grants 309961/2013-0 and 476490/2013-8.

This work has been partially supported by the Brazilian agency CAPES.

7. REFERENCES

Ansys. Fluent 18.0, 2017a. “Customer Guide”, Ansys Inc..

Ansys. Fluent 14.0, 2017b. “Theory Guide”, Ansys Inc..

Bennett, B.A.V., McEnally, C.S., Pfefferle, L.D., Smooke, M.D., 2000. “Computational and experimental study of axisymetric coflow partially premixed methane/air flames”. *Combustion and Flame*, Vol. 123, p. 522-546.

Cao, S., Ma B., Bennett, B.A.V., Giassi, D., Stocker, D.P., Takahashi, F., Long, M.B., Smooke, M.D., 2015. “A computational and experimental study of coflow laminar methane/air diffusion flames: Effects of fuel dilution, inlet velocity, and gravity”. *Proceedings of the Combustion Institute*; Vol. 35; p. 897-903.

Cassol, F., Brittes, R., França, F.H.R., Ezekoye, O.A., 2014. “Application of the weighted-sum-of-gray-gases model for media composed of arbitrary concentrations of H2O, CO2 and soot”. *International Journal of Heat and Mass Transfer*, Vol. 79, p. 796-806.

Celik, I.B., Ghia, U., Roache, P.J., Freitas C.J., Coleman, H., Raad, P.E., 2008. “Procedure for estimation and reporting of uncertainty due to discretization in CFD applications”. *ASME Journal of Fluid Engineering*, Vol. 130, p. 07800-1 – 078001-4.

Connelly, B.C., Long, M.B., Smooke, M.D., Hall, R.J., Colket, M.B., 2009. “Computational and experimental investigation of the interaction of soot and NO in coflow diffusion flames”. *Proceedings of the Combustion Institute*, Vol. 32, p. 777-784.

Demarco, R., Nmira, F., Consalvi, J.L., 2013. “Influence of thermal radiation on soot production in laminar axisymmetric diffusion flames”. *Journal of Quantitative Spectroscopy & Radiative Transfer*, Vol. 120, p. 52-69.

Dorigon, L.J., Duciak, G., Brittes, R., Cassol, F.,Galarça, M., França, F.H.R., 2013. “WSGG correlations based on HITEMP2010 for computation of thermal radiation in non-isothermal, non-homogeneous H2O/CO2 mixtures”. *International Journal of Heat and Mass Transfer*, Vol. 64, p. 863-873.

Hottel, H.C., Sarofim, A.F., 1967. *Radiative Transfer*. McGraw-Hill, New York.

Liu, F., Guo, H., Smallwood, G.J., 2004. “Effects of radiation model on the modeling of a laminar coflow methane/air diffusion flame”. *Combustion and Flame*, Vol. 138, p. 136-154.

Ma, B., Cao, S., Giassi, D., Stocker, D.P., Takahashi, F., Bennett, B.A.V., Smooke, M.D., Long, M.B, 2015. “An experimental and computational study of soot formation in a coflow jet flame under microgravity and normal gravity”. *Proceedings of the Combustion Institute*, Vol. 35; p. 839-846.

Maurente, A., Bruno, A.B., França, F.H.R., Howell, J.R., 2017. "Non-dimensional wavenumber in fullspectrum k-distribution computations with or without a reference state". Journal of Quantitative Spectroscopy and Radiative Transfer, Vol. 196, p. 222-229.

McEnally, C.S., Schaffer, A.M., Long, M.B., Pfefferle, I.D., Smooke, M.D., Colket, M.B., Hall, R.J., 1998. "Computational and experimental study of soot formation in a coflow, laminar ethylene diffusion flame". *Twenty-Seventh Symposium (International) on Combustion/The combustion Institute*, p. 1497-1505.

Modest, M.F., 1991. "The Weighted-Sum-of-Gray-Gases model for arbitrary solution methods in radiative transfer". *Journal of Heat Transfer*, Vol. 113, p. 650-656.

Roache, P.J., 1994. "Perspective: a method for uniform reporting of grid refinement studies". *ASME Journal of Fluid Engineering*, Vol. 116, p. 405-413.

Sivathanu, Y. R., Gore, J. P., 1997. "Total radiative heat loss in jet flames from single point radiative flux measurements". *Combustion and Flame*, Vol. 94, p. 265–270.

Smooke, M.D., Hall, R.J., Colket, M.B., Fielding, J., Long, M.B., McEnally, C.S., Pfeffere, L.D., 2004. "Investigation of the transition from lightly sootin towards heavily sooting co-flow ethylene diffusion flames". *Combustion Theory and Modeling*, Vol. 8, p. 593-606.

Smooke, M.D., Long, M.B., Connelly, B.C., Colket, M.B., Hall, R.J., 2005. "Soot formation in laminar diffusion flames". *Combustion and Flames*, Vol. 143, p. 613-628.

Solovjov, V.P., Andre, F., Lemonnier, D., Webb, B.W., 2017. "The rank correlated SLW model of gas radiation in non-uniform media". *Journal of Quantitative Spectroscopy and Radiative Transfer*, Vol. 197, p. 26-44.

8. RESPONSIBILITY NOTICE

The authors are the only responsible for the printed material included in this paper.